Chapter 5

Roller Facility Tests

A second set of experiments was run at American Roller Company Research and Development facility on plastic webs running over a rotating roller. A test stand consisting of a backplane and movable rollers was used to test web heating under dynamic conditions. The dynamic conditions allowed for the effect of air entrainment of the web to be measured. The measurement of plastic temperatures during the dynamic tests on the roll test stand required non-contact temperature measurement methods. From the web inlet and outlet and roller temperature measurements, the contact resistance of the web roller interface was calculated. Both infrared thermocouples and infrared pyrometers have been used in non-contact applications. Due to the thinness of the plastics used in this study, they are translucent to some of wavelengths used by the infrared sensors. The methods used in this study to circumvent these problems are explained in this chapter.

5.1 Radiation Basics

All objects that are at a temperature above absolute zero emit thermal radiation. Radiation can be explained in two ways, as particles or as waves. As a particle, radiation is quantified as emitted photons, which are massless packets of energy. As a wave, radiation is

modeled with a characteristic frequency and wavelength, related to the speed of light such that:

$$c = \frac{l}{n} \tag{5.1.1}$$

The actual production of radiation is due to the vibration of matter, both on a molecular and atomic basis. The variety of particle masses, vibration modes, and interactions with other particles are responsible for the continuous spectrum of radiation that can be produced. The spectrum of wavelengths taken by radiation in general is infinite, but the wavelength range of thermal radiation is narrow. Gamma rays have the shortest wavelengths, less than 10^{-4} μm, and microwaves have the largest from 10^{3} μm and up. Thermal radiation has the wavelength range from 10^{-1} to 10^{2} μm. The visible wavelengths are a further subset of this, from 0.4 to 0.7 μm.

Infrared radiation extends from the long limit of visible radiation (the color red) through the extent of the thermal wavelengths.

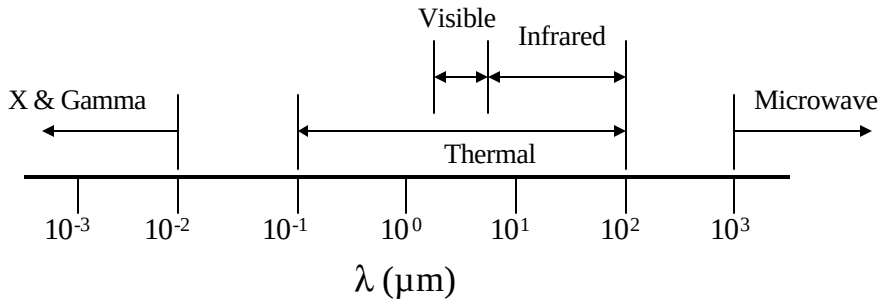

Figure 5.1.1: Condensed Electromagnetic Spectrum.

Radiation is produced in the molecular layers near the surface, and for most cases it can be viewed as a surface phenomenon. This allows radiation exchange to be modeled as occurring between two or more surfaces. However radiation is not a surface phenomenon when it is produced from an absorbing and emitting medium such as a hot gas or a plastic melt. The plastics used in this study are on the borderline between being able to view radiation as a surface mechanism, and different methods are developed to permit the use of radiation as a surface phenomenon.

The first step in the modeling of radiation is to approximate the radiation emitter as a 'black body' emitter. A black body emitter has three necessary and sufficient characteristics.

1. A black body must absorb all incident radiation from other objects.
2. It must emit the maximium amount of energy possible for any given temperature and wavelength.
3. The black body must be a diffuse emitter and emit equally regardless of direction.

Max Planck (1959) determined the relation between black body radiation emission and wavelength.

$$E(l,T) = \frac{C_1}{l^5 \cdot (e^{\frac{C_2}{l \cdot T}} - 1)} \tag{5.1.2}$$

where: $C_1 = 2 \cdot p \cdot h \cdot c_o^{\ 2} = 3.742 \cdot 10^8 W - mm^4 / m^2$ (5.1.3)

and: $C_2 = \frac{h \cdot c_o}{k} = 1.439 \cdot 10^4 mm - K$ (5.1.4)

The constants *h* and *k* are the Planck and Boltzman constants respectively. C_o is the speed of light in a vacuum. When the blackbody emission at various temperatures is plotted, the importance of Plank's distribution becomes clear. The distribution in the wavelengths for thermal radiation is shown below.

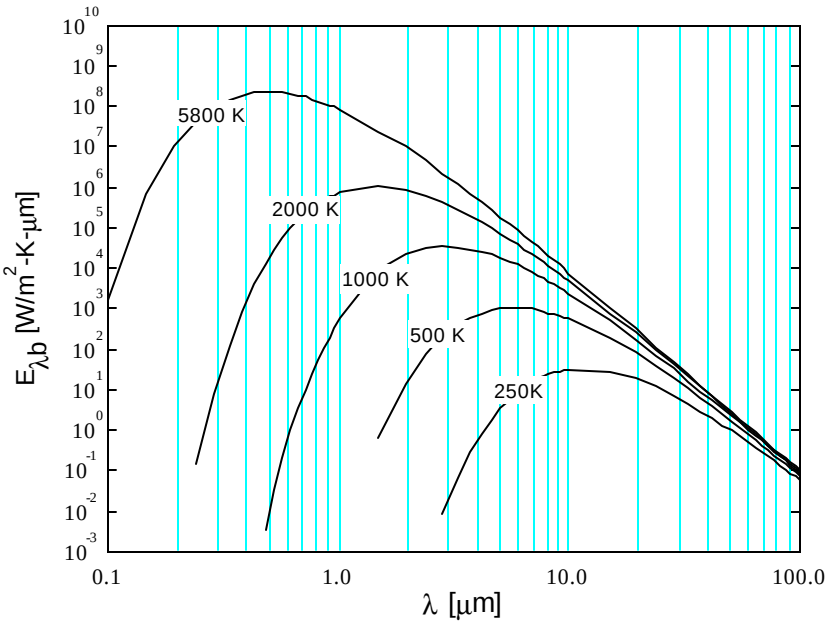

Figure 5.1.2: Plancks' Energy Distribution for Blackbodies.

As can be seen from figure 5.1.2, the characteristic radiation emitted from a blackbody solely depends on its temperature, and each temperature produces a different signature spectrum. The radiation signature is useful because it can be used to find the temperature of a emitting body from a know radiation measurement, assuming a perfect emitter.

Real surfaces complicate the radiation picture. Real surfaces do not absorb all incoming radiation, and do not emit as much radiation as a perfect blackbody would at the same temperature. The plastics used in this study are transparent over certain radiation wavelengths, and are poor emitters. The incoming irradiation on the plastic can be reflected, absorbed or transmitted through the plastic, as indicated in figure 5.1.3

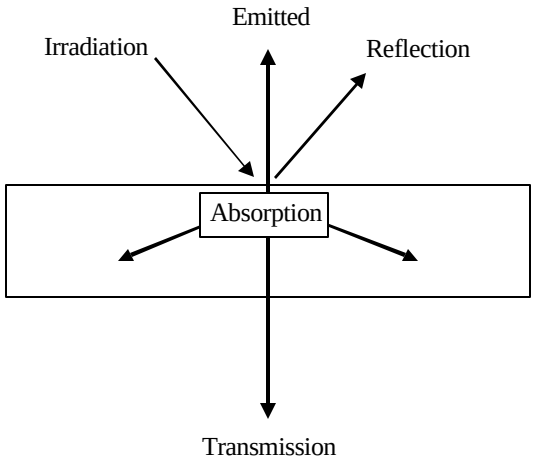

Figure 5.1.3: Radiation Processes in a Semi-Transparent Medium.

The two plastics used in the dynamic roll test study, the 0.127 mm polyester and 0.508 mm PVC, were partially translucent to thermal radiation and care had to be taken to maximize the signal to noise ratio sent to the temperature measurement device.

5.2 IR Pyrometers

Non-contact temperature sensors generally take two forms, infrared pyrometers and infrared thermocouples. While they can be used in similar ways, they work on different principles.

Infrared thermocouples consist of a thermopile and a focusing aid enclosed in housing. A thermopile consists of multiple thermoelectric junctions joined in series. Common thermocouple junctions such as type J or K are commonly used. The series connection of the separate junctions produces a voltage gain, and the thermopile can be tuned to a desired response by controlling the number of junctions and the junction type. The temperature of the hot object is inferred by the voltage response of the thermopile when aimed at the object. The radiation from the hot object heats the thermopile, which then produces a voltage potential. The infrared thermocouple measures temperature by the voltage response of the thermoelectric junction.

An infrared pyrometer uses a radiation sensitive transducer, typically a silicon photodiode, to measure the radiation flux emitted by an object. Then from both the spectral sensitivity of the transducer and Plancks' temperature distribution, the temperature of the object being sensed is determined. Usually a focusing mechanism acts as a selective filter to optically limit the sensed radiation to a narrow acceptance cone.

Common pyrometer spectral sensitivities range from a relatively wide band of 2 – 20 μm or of 8-14 μm to narrow band sensors with sensitivities of 7.95 ± 0.05 μm. The sensitivity range generally needs to be matched to the application. Two wide band infrared pyrometer were used in this study. The D501 handheld model for Exergen Corporation was sensitive in the 2-20 μm range, and the Raytek MX 4 + model was more selective, with a spectral sensitivity from 8-14 microns.

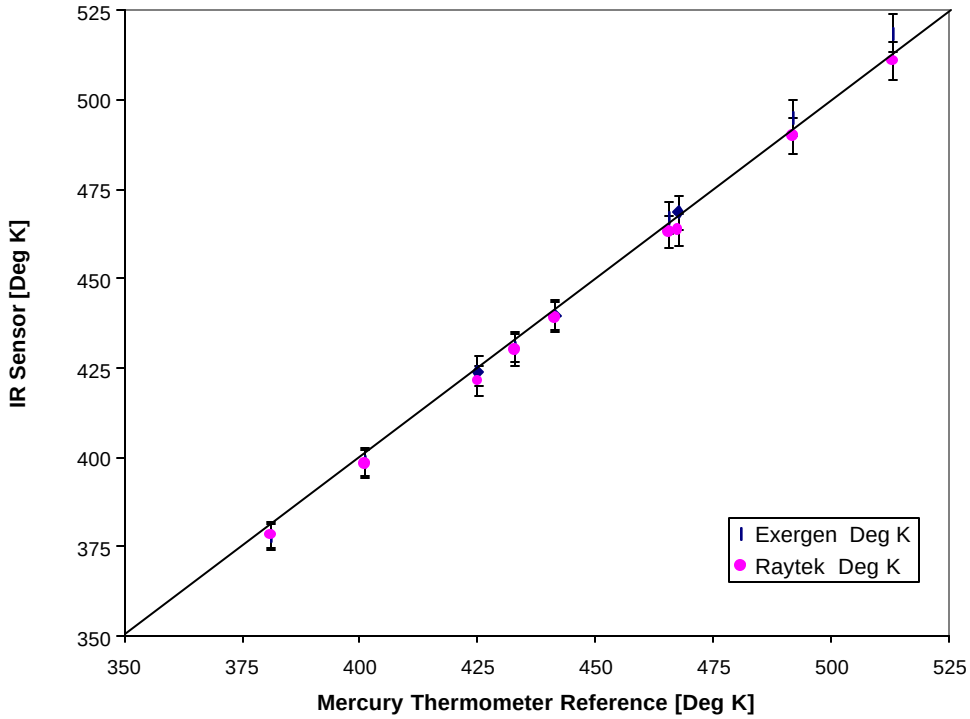

Figure 5.2.1: Raytek and Exergen Reading vs. Mercury Thermometer Reference.

The two thermometers were compared with the mercury thermometer in a melting point apparatus. The apparatus was painted with carbon black grill paint and an emisivity of 0.98 was assumed. Figure 5.2.1 shows the measurements as well as error bars based on the 1 % stated error for both sensors. The measured accuracy of the Exergen and the Raytek thermometer were within manufacturer specifications.

5.3 Data Reduction Method - PVC

The measurements from the roll tests were used to calculate the contact resistance for the specified web speed, material and interface pressure conditions. The two-dimensional

transient finite difference model explained in chapter 4 was used to calculate the contact resistance of each run at the test facility. The contact resistance was modeled as a conduction resistance node between the surface temperature of the roller and the surface of the web in contact with the roller.

The data was taken by keeping the speed constant and varying the tension on the web. Web tension had a linear effect on the interface pressure. After each set at a specific speed, the machine was run without heater power to allow the web and guide rollers to cool off. 0.508 mm PVC is completely opaque in the range of wavelengths used by the Raytek sensor, which leads to a higher accuracy in the measurements.

For each run during the roll testing, temperatures were measured at three points. The temperature of the roll was measured at the bottom of the roll, away from the web contact zone. This was the most accessible place to take the measurements. As the circumferential variance in the surface temperature was small, the measurements represented an average temperature. The inlet temperature of the web was measured immediately before the web contacted with the heater roller.

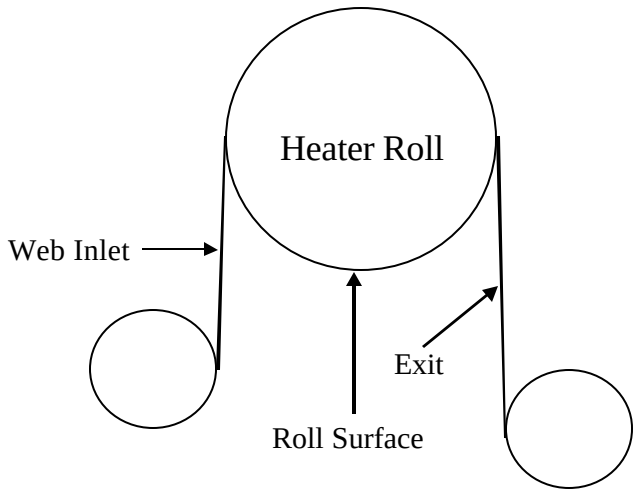

Figure 5.3.1: Temperature Measurement Locations on Roll Test Stand

As seen in figure 5.3.1, the exit temperature of the web was measured a close as possible to the exit spot of the web, about 0.20 m from the roller exit. The exit temperature was also measured from the side of the web that was in contact with the heater roller. This became important with the thicker web used in the roll stand tests, as there was a temperature difference across the thickness of the web. The wrap angle of the test apparatus was approximately 180 degrees, giving a contact length of the interface was 0.48 meters, for the 0.305 meter external diameter of the roll. The web width was 0.152 m, and the temperature of the heater roller was assumed constant across its axial face.

The finite difference program was used to find the value of the contact resistance between the web and the roller that predicted the measured response of the plastic. Given the nature of the steady periodic solution and the fact that the web cooled slightly between leaving the roller and the measurement point, the solution time was lengthy.

The web exit temperature was not measured at exactly the separation point between the web and the roller, and the temperature of the inside surface of the web decreased for two reasons. The greatest temperature change was due to the internal conduction through the web. The web temperatures were not uniform across the web thickness while the web was passing over the roller, and after leaving the roller, the energy was redistributed. The energy gained by the web was absorbed by contact layer of the web and then conducted to the layers of the web away from the surface of the roller. At the measurement point the web had not completely settled to its new temperature distribution.

Figure 5.3.2 Shows the model temperatures for a given web condition and measured temperatures. The measured and predicted surface temperature of the heater roller is also shown.

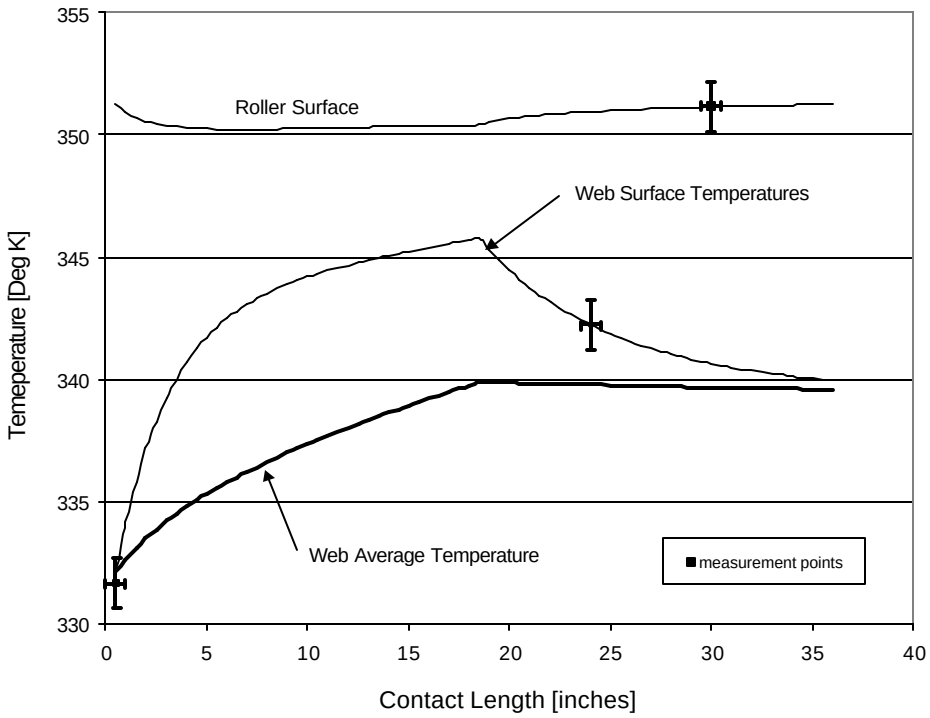

Figure 5.3.2: Temperature Measurements and Predicted Temperature Responses for 0.508 mm PVC at 1m/s. $R_{tc} = 0.010\ m^2\text{-}K/W$

The three measured temperatures used in the calculation are shown on the above plot. The inlet temperature of the web, the roller surface temperature and the outlet temperature are marked. A representative case for the 0.508 mm PVC plastic is shown. The web speed is 1 meter per second. The calculated temperature profiles are shown for the surface temperatures of the roll and web. As the contact surface temperature of the web was measured and was noticeably different from the average web outlet temperature, the surface temperature was input into surface contact node of the finite difference code as the boundary condition used in the run. This was consistent with the definition of the contact resistance as:

$$R''_{tc} = \frac{T_{roller,surface} - T_{web,surface}}{q''_{transferred}} \tag{5.3.1}$$

The contact resistance measured in the PVC tests were higher than the values measured with the transient temperature blocks technique. The average results for the roll tests with the Raytek sensor was 0.0010 m^2-K/W vs. 0.0008 m^2-K/W for the smooth plastics and stationary tests. Given the relative error in both sets of measurements, it is hard to determine the significance of the difference. The results are shown in figure 5.3.2.

The results show little effect of web speed on the measured contact resistances. While the contact resistance's measured at 0.5 m/s were the lowest taken, the data taken at the highest speeds were not the highest contact resistances measured. It was expected that at higher speeds, there would be more air entrainment and higher contact resistances. This was not seen in the measurements, due to the high relative error in the measurements.

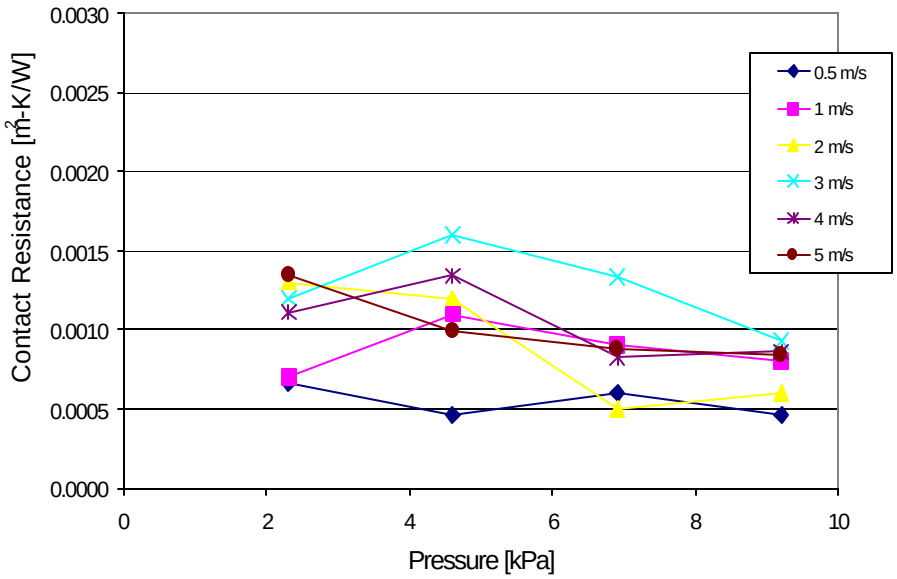

Figure 5.3.3: Contact Resistance Results for 0.508 mm PVC & Raytek Sensor

As with the stationary tests, there is no consistent variation in measured resistance with pressure. Pressure is expected to be a factor in determining the actual contact resistance, but the error in the study and the small range of pressures examined in the study prevent the effect from being shown.

An error analysis showed the effects of the errors in the temperature measurements. EES was used to estimate the magnitude of the experimental error using error propagation of measurement uncertainties. The 0.5 m/s, 1 m/s and 5 m/s runs were used to estimate the uncertainty in the contact resistance due to measurement errors in the temperature. The temperature measurements on the incoming, outgoing and roll temperatures were estimated to have a ±1.5° K accuracy. The calculated errors are characteristic of the dynamic roll tests.

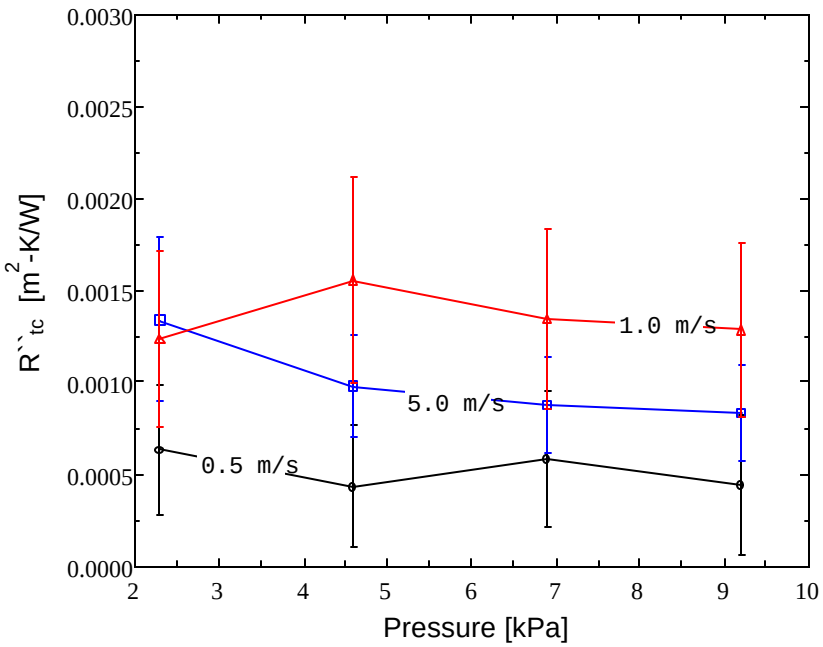

Figure 5.3.4: Error analysis of 0.508 mm PVC Measurements.

As seen in figure 5.3.4 the temperature measurement errors resulted in a ±0.0005 m^2-K/W error in the contact resistance. With the assumed error of ± 1.5° K, the error bars of all of the runs overlap, implying that when the error is included all of the data is indistinguishable. The large error is evident in the fact that the contact resistance measured for the 5 m/s runs is less than measured in the 1 m/s runs.

Measurements were also taken with the wider band Exergen Sensor. Given the need for the Exergen to almost touch the web, and the tight confines of the roll test stand, it became dangerous to hold the sensor at high speeds. For this reason the speeds were limited to less than 2 m/s. The pressures used were identical to the measurements taken with the

Raytek sensor. The spectral transmissivity of PVC over the sensitivity range of the Exergen sensor varies from 50 to 0%, which introduces additional error in the measurements.

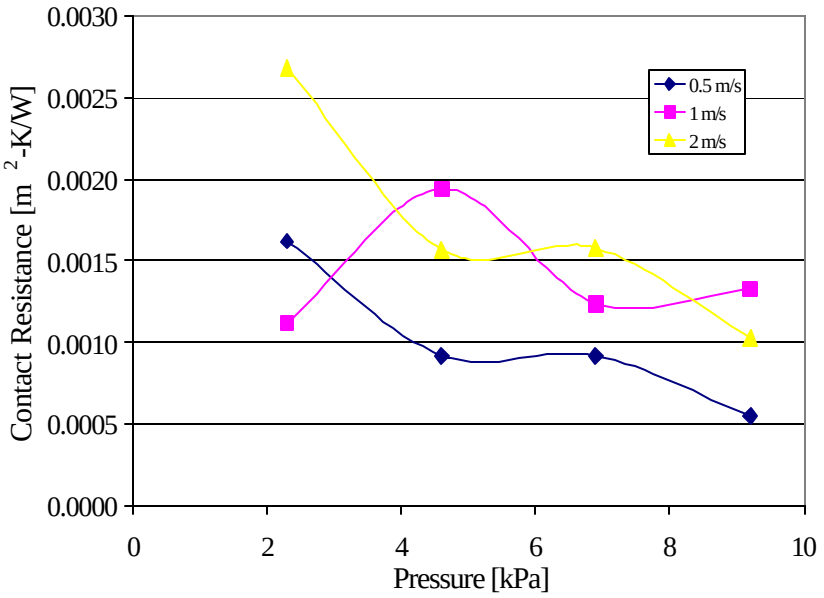

Figure 5.3.5: Contact Resistance Results for 0.508 mm PVC & Exergen Sensor

The data taken with the Exergen sensor was reduced with the finite difference model, like the Raytek data. From figure 5.3.5 there appears to be both an effect of interface pressure and web speed, which would be expected. However the determined contact resistances are much higher than determined with the Raytek sensor.

5.4 Data Reduction Method – Polyester

The data reduction technique for the polyester was similar to the PVC runs. However due to the high transmisivity of the plastic different methods were used to improve the signal to noise ratio of the measurements. The primary method was to isolate the polyester web

from all background radiation. This was done by placing a highly reflective mirror directly behind the web, and placing the acceptance cone of the radiation sensor as close as possible to the surface of the plastic. The mirror itself was made from glass with a thin layer of gold and another protective coating over the gold. Gold has a high reflectivity, approaching 98% in the infrared range used by both sensors.

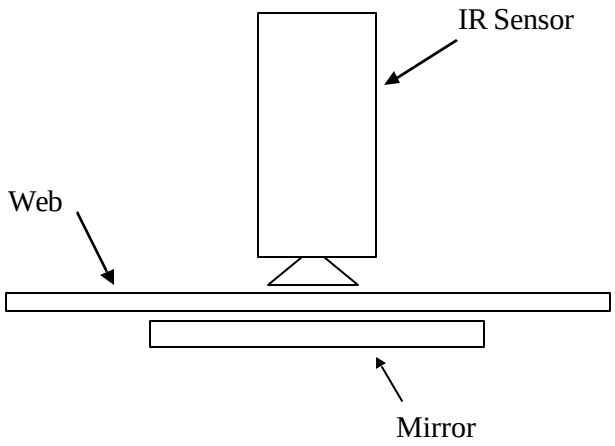

Figure 5.4.1: Measurement Technique for 0.127 mm Polyester.

The sensors were calibrated using an oven and a mercury thermometer. The web, with the mirror placed behind it, was placed in an oven and left to come into equilibrium with the temperature of the oven. Then the door of the oven was opened, and a reading was quickly taken of the plastic. This was repeated over the temperature range expected in the experiments. A graph of the readings vs. oven temperature is shown in figure 5.4.2.

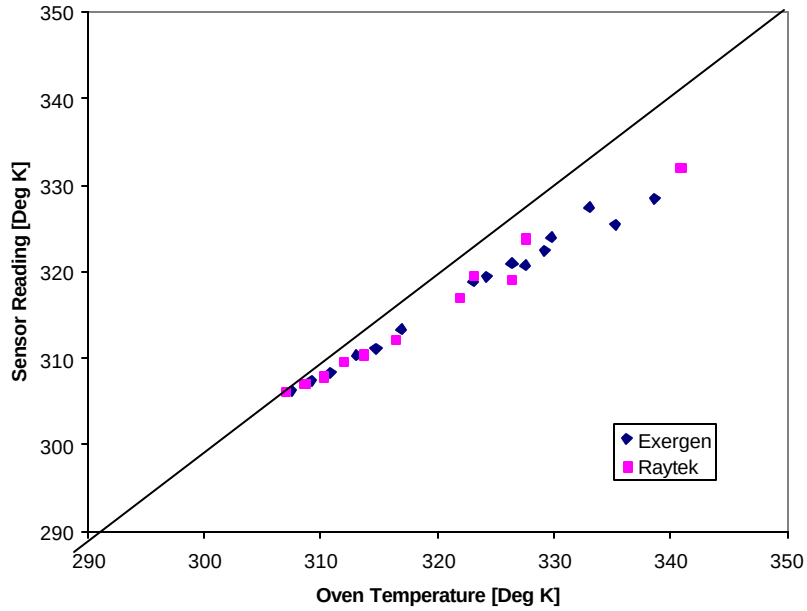

Figure 5.4.2: Oven Calibration Data for 0.127 mm polyester plastic

The air temperature in the oven was measured with a mercury thermometer. From the oven calibration a relative emissivity for the plastic was calculated. The emissivity calculated was for the specific plastic, with a mirror behind the plastic blocking all background radiation. It was not so much an emissivity as conventionally defined by radiation principles but a correction factor to convert a reading temperature to an actual temperature. The correction emissivity was defined as:

$$T_{actual} = \frac{(T_{reading} + 273.1)}{\sqrt[4]{e}} - 273.1 \qquad (5.4.1)$$

Where the reading and actual temperatures are in degrees Celsius. The ‘best fit’ emissivity for the Raytek and the Exergen was very close, at 0.94 and 0.95 respectively.

Typical emisivities for translucent plastics are 0.1-0.4, but the correction emisivity used in these tests includes radiation from both sides of the plastic. This is due to the mirror reflecting back the radiation from the side of the plastic away from the sensor.

For all of the actual roll tests measured with the 0.127 mm polyester web, the mirror was placed directly behind the web from the sensor. The sensor and the mirror were placed as close as possible to the web, as shown in figure 6.4.1. The readings from both sensors were then corrected with the emissivity adjustment. A test of the accuracy correction was then run. The web was run over a heater roller at a very slow speed, approximately 0.05 – 0.10 m/s. This allowed the entire cross section of the web to heat up until it almost reached the actual roller surface temperature. The temperature of the polyester web was then measured, corrected with the equivalent emisivity, and compared with the measured roll temperature. An exact match would mean that the sensors were reading correctly.

As the measurement technique required the placement of the mirror directly behind the web, the measurements were taken almost 0.20 m after the web had left the surface of the roller. Even at the low speeds, the radiation and convection loss to the surroundings was large enough to cool the thin web off in the short distance. The computer model was used to predicted the web heating as it passed over the roller, and the subsequent cooling as it left the roller surface. Convection was considered negligible, and a linearized radiation coefficient was used to estimate the heat loss to the surroundings.

A linearized radiation coefficient was defined as:

$$h_{rad} = e_{web} \cdot s \cdot (T_{web}^2 + T_\infty^2) \cdot (T_{web} + T_\infty) \qquad (5.4.2)$$

and for an epsilon of 0.25 had a value of 2.1 W-m^2/K. The heat loss to the surroundings produced a predicted temperature drop of approximately 1.5° K by the position of the sensor. This is shown in figure 5.4.3. below.

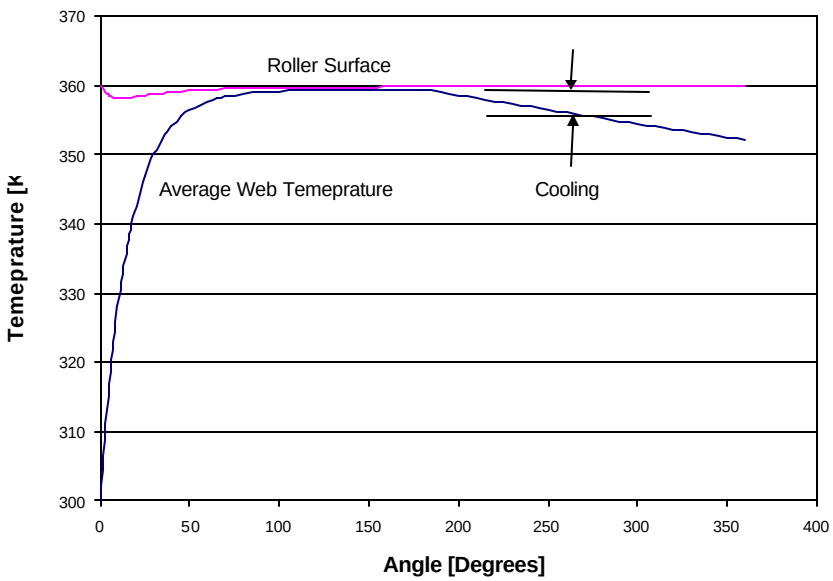

Figure 5.4.3 Web Heating and Subsequent Cooling During Calibration Run. R_{tc} = 0.002 m^2-K/W, 0.10 m/s

The finite difference program was run with the largest contact resistances encountered in the static measurements. A second correction factor was developed to account for the cooling of the web before it was measured. The cooling correction factor was

developed by parametrically studying the effect of different roller temperatures on the cooled temperature at the measurement point. A first order polynomial was fit to the cooled plastic temperature vs. roller temperature. This assumed that the web actually reached the roller surface temperature. Based on predictions by the finite difference program, the web approached the roller surface temperature to 0.2° K.

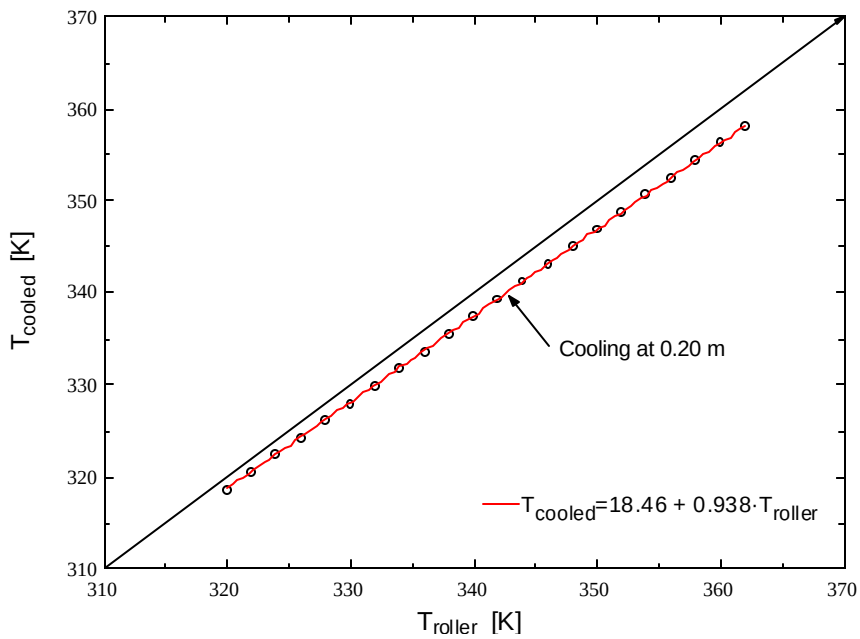

Figure 5.4.4: Predicted Cooling for 0.173 mm polyester Web at 0.5 m/s. 0.20 m After Leaving Roller Surface.

Given the above correlation, the results of the slow web passing over the roller can be compared with the measured roller temperature. The roll temperature was measured with an infrared pyrometer, and used as a reference. When this was done, figure 5.4.5 was the result. Figure 5.4.5 shows the corrected web temperature at the measurement location for a known

(relatively) roll surface temperature. The effect of both the emisivity and the cooling correction is shown.

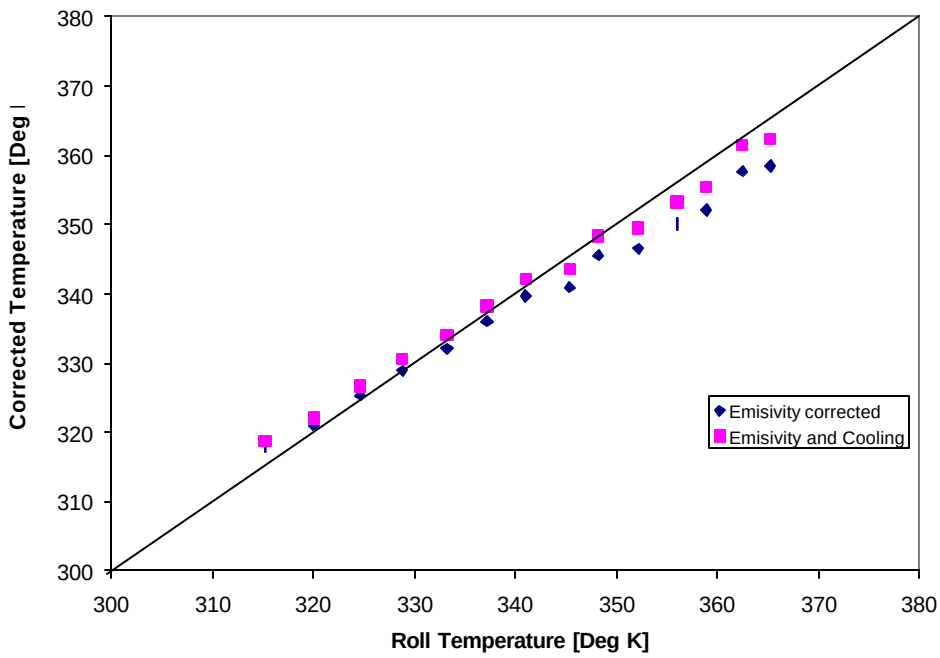

Figure 5.4.5: Calibration Results for 0.127 mm Polyester Plastic and Exergen Sensor.

When corrected, the sensors read radiation signal from the 0.127 mm polyester show that the temperature is very close to the roll temperature.

Once the calibration curves had been made, the actual experiments on the roll test stand were performed. In all cases the contact resistance was determined as a function of web speed and interface pressure. The polyester plastic was tested first, and the results are shown in figure 5.4.6 below. There is a dependence on interface pressure, and a web speed effect. The highest contact resistances were measured at the lowest web speed 0.5 m/s.

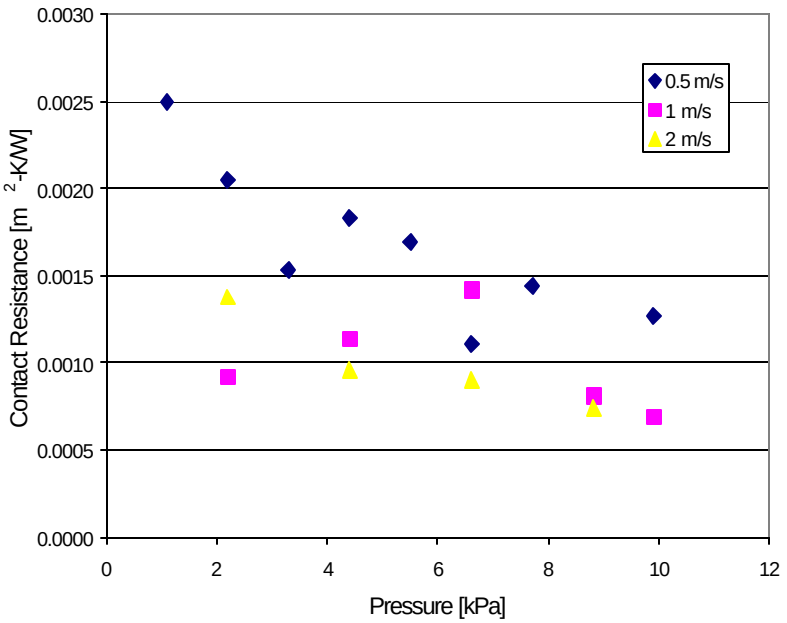

Figure 5.4.6: Contact Resistance Results for Polyester & Exergen Sensor

The pressure effect may be due to more to web alignment problems than microscopic web and roller surface roughness characteristics. Macroscopic errors would result of the roller immediately preceding the heater roller was not exactly parallel with the heater roller. If the two rollers were not in alignment then the web would not see full contact with the heater roller, and be only heater for part of the nominal contact area. The error in the measured contact resistances are shown in figure 5.4.7 below, only the error bars for the 0.5 m/s and 2 m/s case are shown.

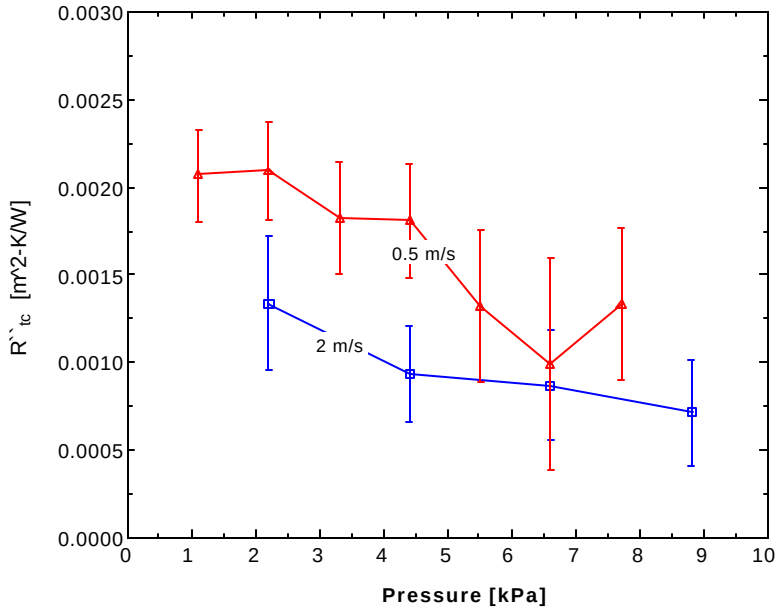

Figure 5.4.7: Error analysis for 0.127mm Polyester & Exergen Sensor

The results obtained with the Raytek sensor and the 0.127 mm polyester were unreliable. The Raytek sensor measurements were not repeatable when attempting calibration in the oven tests with the 0.127 mm polyester. Without a calibration curve, the base temperature measurements could not be considered accurate to base the contact resistance results on.

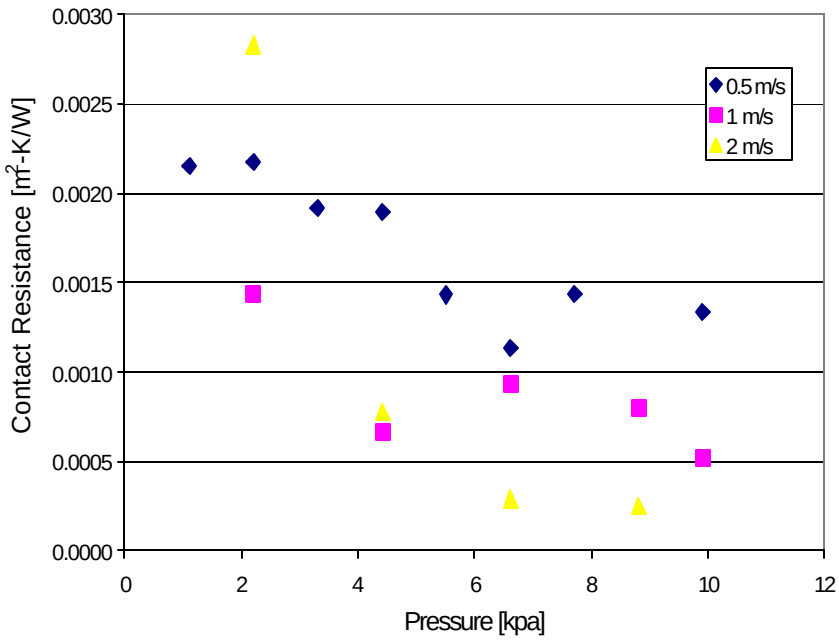

Figure 5.4.8: Contact Resistance Results for Polyester & Raytek Sensor

Even with outliners removed, the range in the measurements is large, around 0.015 m^2-K/W. The bulk average is close to the other measurements, around 0.0010 m^2-K/W.

5.5 Comparison with Lumped Capacitance Results

The contact resistance measurements from the dynamic tests compare favorably to the static blocks tests discussed in chapter 4, within experimental error. For the smooth plastics (Polyester, PVC and Polypropylene) the average for all pressures and speeds was 0.0008 m^2-K/W and 0.0010 m^2-K/W for the static and dynamic tests respectively. The embossed polyethylene was not tested dynamically due to its very high transmisivity over then range of the infrared pyrometers. While the measurements did not show the expected increase in contact resistance with web speed, a similar lack of dependence in

the contact resistance on web speed was shown in the results presented by Kerekes 1980. As Kerekes measurements were taken using a thicker paper web, the infrared measurements were accurate.

The closeness of the measurements validates the usefulness of using static measurements to predict the contact resistance of roller-web interfaces. In general, from the experimental results presented in this thesis the static measurements will be more accurate than the dynamic measurements due to the high experimental errors inherent in the infrared pyrometer process. Even if narrow band infrared pyrometers are used, greater accuracy can be achieved with static measurements.